J Therm Anal Calorim (2016) 125:121–128
DOI 10.1007/s10973-016-5373-2

Study on the catalytic effect of diaminoglyoxime on thermal behaviors, non-isothermal reaction kinetics and burning rate of homogeneous double-base propellant

Seied Mahdi Pourmortazavi[1] · Khalil Farhadi[2] · Vahid Mirzajani[2] · Saeed Mirzajani[3] · Iraj Kohsari[4]

Received: 16 November 2015 / Accepted: 25 February 2016 / Published online: 18 March 2016

Abstract This paper reports thermolysis of diaminoglyoxime (DAG) as a ballistic modifier, and its effects on the thermal behaviors, non-isothermal decomposition reaction kinetics, and burning rates of the homogeneous double-base propellant formulations. Thermal analysis studies were performed by thermogravimetric analysis and differential thermogravimetry (TG-DTG) and differential scanning calorimetry techniques. According to the resulted data, it was found that DAG could change the thermal decomposition mechanism function, thermokinetic parameters and kinetic equation of the propellants. Evaluation of DAG as a ballistic modifier in double-base propellant formulations indicated that it brings down the pressure index to 0.068 compared to 0.24 for the control composition in the pressure range 5–7 Mpa. The results showed that the main exothermal decomposition reaction of the propellant sample in the absence of DAG has the mechanism function of $f(\alpha) = \frac{3}{2}(1-\alpha)^{4/3}[(1-\alpha)^{-1/3}-1]^{-1}$ and the kinetic equation of $^{d\alpha}/_{dt} = 1.60 \times 10^{17}(1-\alpha)^{4/3}[(1-\alpha)^{-1/3}-1]^{-1}e^{-2.21\times10^4/T}$, while modified propellant with DAG has a different function mechanism and kinetic equation as following: $f(\alpha) = \frac{5}{2}(1-\alpha)[-\ln(1-\alpha)]^{3/5}$ and $^{d\alpha}/_{dt} = 9.28\times10^{40}(1-\alpha)[-\ln(1-\alpha)]^{3/5}\ e^{-4.66\times10^4/T}$, respectively.

Keywords Diaminoglyoxime (DAG) · Thermal behaviors · Non-isothermal kinetics · Burning rate · Double-base propellant

Introduction

Diaminoglyoxime (DAG) is an explosophoric compound, with the chemical structure illustrated in Scheme 1. The compound is prepared by dehydration of dihydroglyoxime (DHG) in the aqueous sodium hydroxide solution at high temperatures [1–5]. This compound might be utilized as additive in the rocket propellant formulations as coolant [6].

Thermokinetic studies are crucial point in thermal analysis, while the main purpose is definition of the decomposition reaction mechanism and calculating the Arrhenius equation parameters, i.e., activation energy and frequency factor [5, 7–10]. The resulted thermoanalytical data could provide valuable information about shelf-life and safe conditions for storage of the materials [11, 12]. Prediction of these parameters for energetic materials is especially meaningful in order to elucidate miscibility/compatibility and their effects on thermal stability of the resulted composition [5, 13–16].

Until today, thermolysis of DAG and its utilization in the composite double-base propellant have been investigated [11] and the results revealed positive role of this

Electronic supplementary material The online version of this article (doi:10.1007/s10973-016-5373-2) contains supplementary material, which is available to authorized users.

✉ Seied Mahdi Pourmortazavi
pourmortazavi@yahoo.com

[1] Faculty of Material and Manufacturing Technologies, Malek Ashtar University of Technology, Tehran, Iran

[2] Department of Analytical Chemistry, Faculty of Science, Urmia University, Urmia, Iran

[3] Department of Mathematica, Payame Noor University, P.O. Box 19395-3697, Tehran, Iran

[4] Department of Chemistry, Amir Kabir University of Technology, Tehran, Iran

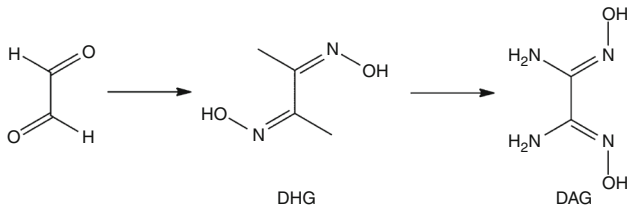

Scheme 1 Synthesis of DAG achieved in two steps from commercially available glyoxanal

compound in modification of double-base propellant. Stoner and Brill [12, 17] observed that thermolysis of DAG at the propellant burning surface leads to formation of a thermally stable melamine. Performing the rapid thermolysis experiments on decomposition reaction of DAG exhibited that formation of highly thermal stable cyclic azines accomplished by the evaluating low molecular weight gases, i.e., NH_3, HCN, CO_2, and N_2O. Meanwhile, Williams et al. [17, 18] found that DAG forms a thermally stable cyclic azine, which is stable up to 700 °C in the superficial reaction layer at the burning surface of the propellant. Formation of these thermal stable products due to the decomposition of the propellant caused retarding the heat transferring from the gas phase to the condensed segment of propellant. In this paper, the influences of DAG as a ballistic modifier on the thermal behaviors, decomposition reaction kinetics and burning rate of the homogeneous double-base (DB) propellant were investigated under the non-isothermal conditions. To the best of our knowledge, there is no information on the decomposition reaction kinetics of the double-base (DB) propellant containing DAG as a ballistic modifier.

Experimental

Sample preparation

DAG as the ballistic modifier of the propellant was synthesized and purified in the organic chemistry laboratory (MUT, Tehran) as proposed previously [19], while the fibrous NC used in the present investigation was of commercial grade with about 12.0 % nitrogen content [20]. The studied double-base propellant sample (control sample or no. P1) was containing of 56 % (mass fraction) NC, 30 % NG, 3 % centralite II, 7 % diethyl phthalate, 4 % other assistant reagents. The propellant sample modified with DAG (no. P_2) was composed of similar components, while 2 % DAG was added and the NC content was reduced to 54 %. The details of the propellant formulations are presented in Table 1. The propellant samples were prepared by a solvent-less double-base propellant extrusion technique, including slurry mixing, rolling, and extruding [9, 17, 21].

Table 1 Percentage composition of various propellant ingredients in samples

Ingredients	Percentage	
	P_1	P_2
Nitrocellulose (NC)	56	54
Nitroglycerine (NG)	30	30
Diethyl phthalate (DEP)	7	7
Centralite II (C2)	3	3
Diaminoglyoxime (DAG)	–	2
other assistant reagents	4	4

Instruments and experimental conditions

Infrared spectrum was obtained with a FT-IR spectrophotometer (Perkin-Elmer 1600) using KBR pellets. Analyses for C, H, and N determination were carried out on a Carlo Erba 1108 Elemental Vario EL analyzer. Thermal behaviors of propellant samples were analyzed by differential scanning calorimeter (DSC) and thermogravimetric analysis (TG). The thermal analyses were carried out on a Mettler TA4000 thermal analyzer and a DSC 1 (Mettler Toledo Co., Switzerland), respectively. The operating conditions of TG analyses were as follows: about 3 mg as the sample mass; purging of N_2 gas with the flowing rate of 80 mL min^{-1}; heating rates (β) of 10 °C min^{-1} in a temperature range of 50–600 °C using an α-Al_2O_3 crucible. The operating conditions of DSC analyses were included: about 1.5 mg as the sample mass; 50 mL min^{-1} as flowing rate of N_2 purging in a temperature range of 50–500 °C using an α-Al_2O_3 crucible; heating rates of 3, 5, 7, and 9 °C min^{-1}. The burning rates of propellant samples under different pressures were determined in an indigenously fabricated Crawford Bomb strand-burner equipment [15, 17].

Results and discussion

Characterization of DAG

As seen in Fig. 1, the room temperature FTIR spectrum of pure DAG in KBr matrix shows absorption bands corresponding to N–O bond of oxime (951.78 cm^{-1}), $-NH_2$ group (3368.79, 3470.35 and 1680.8 cm^{-1}), and –OH group (2800–3300 and 1447.74 cm^{-1}), while the absorption band observed at 1652.41 cm^{-1} may be attributed to C=N bond. The resulted data from IR analysis of DAG are

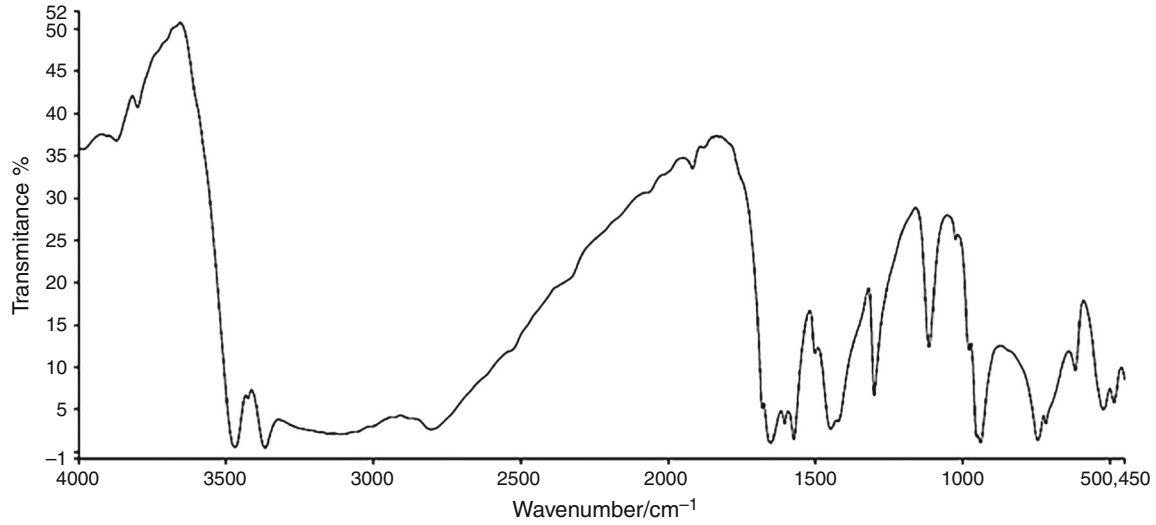

Fig. 1 FT-IR analysis of the synthesized DAG

Table 2 IR pattern analysis of the synthesized DAG

Functional group	Wavenumber/cm^{-1}	Intensity[a]
N–H_2	3368.79, 3470.35, 1680.8	vs, B
O–H	2800–3300, 1447.74	m, B
C=N	1652.41	S
N–O	951.78	S

[a] The IR broad band intensity expression: *vs* very strong, *s* strong, *m* middle, *B* broad

listed in Table 2. Elemental analysis (%), calcd. for $C_2H_6N_4O_2$ (%): C, 20.34; H, 5.12; N, 47.44. Found (%): C, 20.54; H, 5.20; N, 47.36.

Thermal properties of DAG

The DSC curve of pure DAG is given in Fig. 2. According to the DSC data, an endothermic peak was observed around 200 °C corresponding to the melting point of DAG. However, DAG was decomposed exothermally at 205.5 °C, after it is melting at the temperature of 200 °C [5].

Thermal behavior of the propellant in the presence of DAG

The TG-DTG curves of the control propellant (sample P_1) and the DAG modified propellant (sample P_2) at the heating rate of 10 °C min^{-1} are shown in Fig. 3. Also, the DSC curves at the heating rates of 3, 5, 7 and 9 °C min^{-1} for both samples are presented in Figs. 4 and 5. As seen in Fig. 3, there are two mass loss stages in the TG curve of the propellant samples. Meantime, two exothermic peaks were observed in the corresponded DTG curves. TG curves of

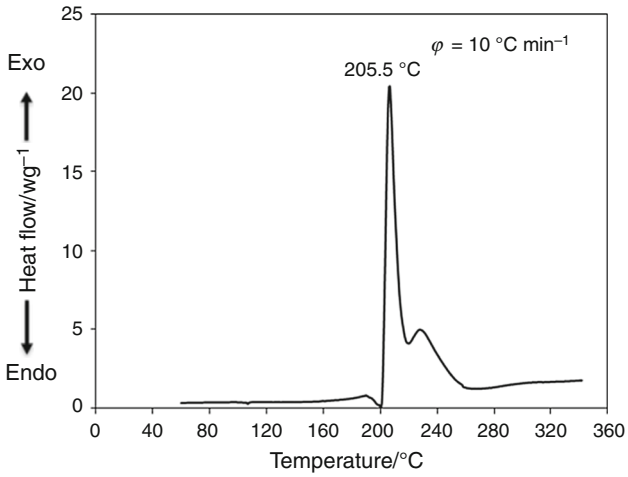

Fig. 2 DSC curve for pure DAG

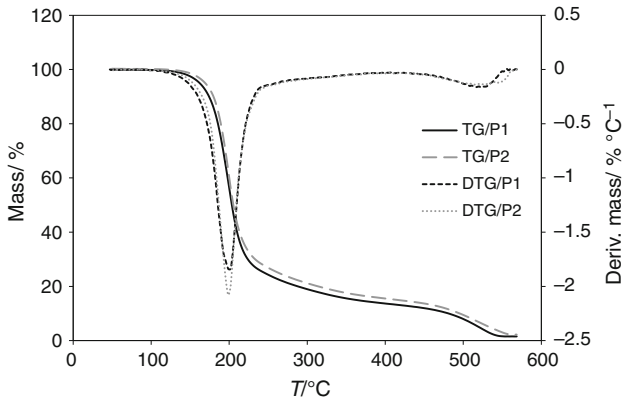

Fig. 3 TG-DTG curve for the control propellant (sample P_1) and DAG modified propellant (sample P_2) sample mass about 3 mg; heating rate 10 °C min^{-1}; N_2 atmosphere

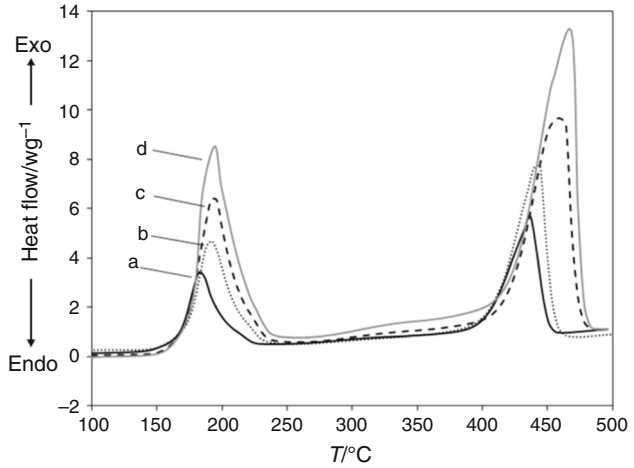

Fig. 4 DSC curves of the control propellant (sample P_1) at different heating rates (°C min^{-1}): (*a*) 3; (*b*) 5; (*c*) 7; (*d*) 9

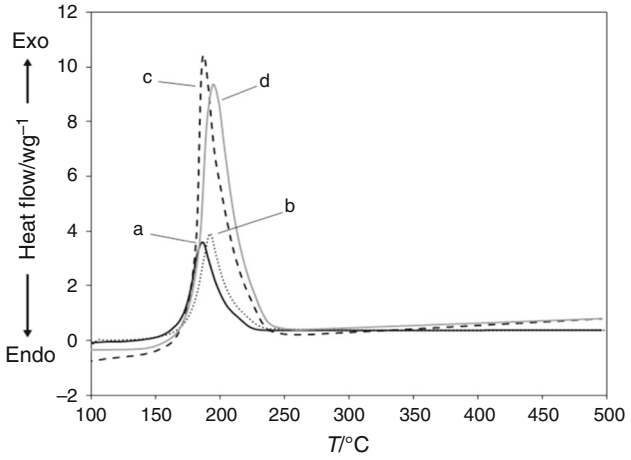

Fig. 5 DSC curves of the DAG modified propellant (sample P_2) at different heating rates (°C min^{-1}): (*a*) 3; (*b*) 5; (*c*) 7; (*d*) 9

both samples, at $\beta = 10$ °C min^{-1}, exhibited that the first stage begins at about 50 °C and stops at about 230 °C, while the peak in the DTG curve was appeared at 199–201 °C accompanying about 84–86 % mass loss, which is close to the total mass of the ester content (NC/NG) of the propellant and hence it likely attributes to the volatilization and decomposition of the NC/NG mixed ester. The second stage begins at about 410 °C and stops at about 550 °C, with the peak in the DTG curve at 508–535 °C, accompanied by 12–13 % mass loss, and it attributes to the reaction of remaining auxiliaries. However, a few remains were observed at the end of the second decomposition stage. In fact, both samples undergo a main exothermic decomposition reaction during their first stage, this results is confirmed by the exothermic peaks observed in the DSC curves of the samples in Figs. 4 and 5. On the other hand, decomposition temperature of the DAG is about 200 °C and this temperature is comparable with the decomposition temperature of the sample at the first stage. On the other hand, the propellant in the presence of DAG decomposes during a single step and the observed exothermic peak in the temperature range of 400–500 °C was not observed. In other word, the presence of the DAG in the formulation has a main influence on the thermal pattern of the propellant and all the ingredients decompose simultaneously during a single peak at a temperature about 200 °C (Fig. 5).

The basic data for the main exothermic decomposition processes of the propellants P_1 and P_2 are listed in Table 3.

Table 3 DSC peak temperature data for the main exothermic decomposition process of the propellant samples

	β/°C min^{-1}	T_e/°C	T_p/°C
P_1	3	172.41	184.3
	5	177.08	190.83
	7	185.45	192.38
	9	185.91	193.1
P_2	3	172.58	183.45
	5	177.18	185.25
	7	181.4	186.26
	9	188.74	187.7

T_e is the onset temperature for the main exothermal decomposition reaction in DSC curve, and T_p is the peak temperature

Calculation of non-isothermal reaction kinetics

Thermal decomposition kinetic, Arrhenius parameters, i.e., the activation energy (E_a) and the pre-exponential constant (A) and the most probable kinetic model function corresponding to the studied propellant samples was explored. The DSC curves resulted from the samples at the heating rates of 3, 5, 7, and 9 °C min^{-1} were employed to examine their compatibility with two well-known integral methods (i.e., Coats Redfern and Flynn–Wall–Ozawa) (Eqs. (1–2) in Table 4] and also two differential methods (i.e., Kissinger and Starink) [Eqs. (3–4) in Table 4] [21–31]. The values of E_a were predicted by the Ozawa method using the isoconversional DSC curves at different heating rates, while the relations between E_a and α for both propellant samples are given in Fig. 6. As seen in this figure, the values of activation energy change slightly in the range of 0.35–0.475 (α) for the control sample (P_1), and 0.225–0.425 (α) for the DAG modified propellant sample (P_2). These ranges were chosen to calculate the non-isothermal reaction kinetics of the samples. Forty-one types of the proposed kinetic model functions in Refs. [32–40] were examined, while the original DSC data were utilized as

Table 4 Kinetic analysis methods utilized for the studied propellant samples

Method	Equation	Method no
Coats Redfern	$\ln\frac{G(\alpha)}{T^2}=\ln\left(\frac{AR}{\beta E_\alpha}\left[1-\left(\frac{2RT_{\exp}}{E_\alpha}\right)\right]\right)-\frac{E_\alpha}{RT}$	(1)
Flynn–Wall–Ozawa	$\ln\beta=\lg\{AE_a/[RG(\alpha)]\}-2.315-0.4567E_a/RT$	(2)
Kissinger	$\mathrm{Ln}\frac{\beta}{T_m^2}=\ln\frac{AR}{E_a}-\frac{E}{RT_m}$	(3)
Starink	$\ln\left(\beta/T_m^{1,92}\right)+1.0008Ea/RT_m=C$	(4)

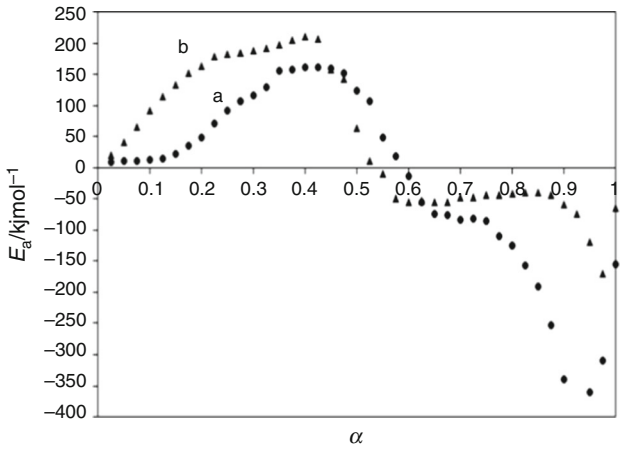

Fig. 6 E_a–α curve for the studied propellant samples (*a*) P_1 and (*b*) P_2)

input of the integral and differential equations. The values of E_a, log A, and the linear correlation coefficient (r) for both propellant samples were calculated and listed in Table 5. The most probable mechanism function could be selected using the better values resulted for r. The data in Table 5 exhibit that the values of E_a and log A computed from the non-isothermal DSC data have good agreement with the calculated values via Flynn–Wall–Ozawa and Kissinger and Starink methods. Therefore, the mechanism function (listed in Table 6) might be determined by substituting the values of E_a/(kJ mol^{-1}) and A/s^{-1} into Eq. (1):

$$\frac{d\alpha}{dt}=Af(\alpha)e^{-\frac{E}{RT}} \quad (1)$$

where $f(\alpha)$ represents the differential model function, t symbolizes time, and R is the universal gas constant. The corresponding kinetic equation to the decomposition reaction of the propellant samples was determined and presented in Table 6. As seen in this table, the addition of DAG to the propellant formulation could change the decomposition reaction mechanism function in comparing with the control propellant.

Thermal safety studies

Self-accelerating decomposition temperature (T_{SADT})

The self-accelerating decomposition temperature (SADT) is defined as the lowest ambient temperature at which an organic substance or self-reactive compound undergoes the self-accelerating decomposition. Determining of this parameter is essential for the safe packaging or transportation purposes in various materials especially in energetics [41]. In this study, the values of the onset temperature (T_e) corresponding to $\beta \to 0$ or T_{e0} were obtained by Eq. (2), and then, the self-accelerating

Table 5 Kinetic parameters of the main exothermic decomposition process of the propellant samples

Method	β/°C min^{-1}	P_1				P_2			
		E_a/kJ mol^{-1}	log$A$/s^{-1}	r	Q	E_a/kJ mol^{-1}	log$A$/s^{-1}	r	Q
Coats Redfern	3	129.95	10.73	0.9969	0.0208	298.85	30.73	0.9934	0.0714
	5	178.05	16.5	0.9998	0.0055	289.98	29.47	0.9930	0.0726
	7	219.52	21.12	0.9986	0.0141	472.9	50.32	0.9950	0.0709
	9	208.88	19.8	0.9982	0.0189	488.47	51.77	0.9968	0.0620
Mean		184.1	17.03	–	–	387.55	40.57	–	–
Kissinger		192.5	19.7	0.9517	0.1721	454.36	50.11	0.9930	0.0674
Starink		192.65	19.72	0.9519	0.1721	454.31	50.10	0.9930	0.0674
Flynn–Wall–Ozawa		190.28	–	0.9552	0.1722	439.15	–	0.9932	0.0674

Q standard mean square deviation

Table 6 Mechanism functions, apparent activation energies and kinetic equations of the studied propellant samples

	$P_1(\alpha = 0.35 - 0.475)$	$P_2(\alpha = 0.225 - 0.425)$
Mechanism function	$G(\alpha) = \left[(1-\alpha)^{-1/3} - 1\right]^2$, $f(\alpha) = \frac{3}{2}(1-\alpha)^{4/3}[(1-\alpha)^{-1/3} - 1]^{-1}$	$G(\alpha) = [-\ln(1-\alpha)]^{2/5}$; $f(\alpha) = \frac{5}{2}(1-\alpha)[-\ln(1-\alpha)]^{3/5}$
Mechanism function no.	9	12
E_a/kJ mol^{-1}	184.1	387.55
Kinetic equation	$d\alpha/dt = 1.60 \times 10^{17}(1-\alpha)^{4/3}[(1-\alpha)^{-1/3} - 1]^{-1} e^{-2.21 \times 10^4/T}$	$d\alpha/dt = 9.28 \times 10^{40}(1-\alpha)[-\ln(1-\alpha)]^{3/5} e^{-4.66 \times 10^4/T}$

Table 7 Thermodynamic data for the studied propellant samples

	P_1	P_2
(T_{e0} or T_{SADT})/K	470.89	430.46
T_{p0}/K	429.20	449.75
T_{bp}/K	437.56	453.64

decomposition temperature (T_{SADT}) for the propellant samples was computed by Eq. (3) [36–40].

$$T_e = T_{e0} + b\beta_i + c\beta_i^2, \quad i = 1 - 4 \tag{2}$$

While, b and c are coefficients.

$$T_{e0} = T_{SADT} \tag{3}$$

The resulted values for the studied propellant samples are given in Table 7.

Critical temperatures of thermal explosion

Critical temperature of thermal explosion (T_b) is defined as the lowest temperature to which a specific charge might be heated without undergoing any thermal runaway [30]. This vital parameter for energetic materials usually is predicted to insure safe processing and storage. T_b could be calculated by considering the ignition theory and corresponding thermo-kinetic parameters, namely the pre-exponential factor, activation energy, and heat of decomposition reaction. The critical temperatures of thermal explosion for both propellant samples were obtained from Eq. (4) [33, 38] and given in Table 7.

$$T_{bp} = \frac{E_0 - \sqrt{E_0^2 - 4E_0RT_{p0}}}{2R} \tag{4}$$

The presented data in Table 7 show that the value of T_{bp} for the DAG modified double-base propellant in comparison with the control sample is high, which confirms the difficulty in happening of transition from thermal decomposition to a thermal explosion in the modified propellant [38].

Burning rate measurement for the studied propellant samples

In order to investigate the possible utilizing of DAG in propellants as the ballistic modifier, the burning rates [u/(mm s^{-1})] of the both control propellant (P_1) and the DAG modified propellant (P_2) were measured and compared at different pressures (P/MPa). The resulted burning rates are listed in Table 8. As seen in this table, the addition of about 2 % DAG to the propellant sample has no significant effect on its burning rate, however brought down the n value. The brought down of the n value from 0.24, for the

Table 8 Effect of DAG on the burning rates (mm s^{-1}) of the studied double-base propellant

Sample	Burning rate/mm s^{-1} at pressure/MPa											*n*-value over pressure range/MPa				
	5	6	7	8	9	10	11	12	13	14	15	5–7	7–9	9–11	11–13	13–15
P1	15.81	16.28	17.16	17.72	18.97	18.49	18.45	18.54	17.93	17.84	17.61	0.24	0.39	−0.14	−0.16	−0.12
P2	14.15	15.36	14.42	16.67	16.95	17.45	17.69	17.63	17.71	18.26	17.54	0.068	0.65	0.21	0.006	−0.06

control sample, to 0.068 for the DAG modified sample in the pressure region of 5–7 MPa was observed. In order to evaluate the effects of DAG as the ballistic modifier on the burning rate of the studied double-base propellant, the pressure exponent (n) of the burning rate (u) was computed. Then, the average values of the catalysis efficiency ($\bar{Z}$) were compared before and after addition of the ballistic modifier into the propellant formulation. To achieve this aim, the values of n and $\bar{Z}$ were obtained by Eqs. (5) and (6) [17, 21, 37, 38]:

$$u_i = aP_i^n, \quad i = 1 - 11 \tag{5}$$

$$\bar{Z} = \sum_{i=1}^{k} \left(u_{II,i} / u_{I,i} \right) / k \tag{6}$$

where a is the coefficient (mm s^{-1} MPa^{-1}).

For the DAG modified propellant: at 5–8 MPa, $u = 4.97P^{0.26}$, $\bar{Z} = 0.9$; at 8–12 MPa, $u = 8.47P^{0.155}$, $\bar{Z} = 1.17$; at 12–15 MPa, $u = 15.7P^{0.024}$, $\bar{Z} = 0.99$.

As seen, addition 2 % DAG as a ballistic modifier to the propellant formulation has no considerable effect on the burning rate, but reduces efficiently the pressure exponent of the double-base propellant.

Conclusions

The ability of DAG as a ballistic modifier for the application in the homogeneous double-base propellant was investigated. Thermo-kinetic results showed that DAG could enhance the enthalpy of decomposition, apparent activation energy, and change the decomposition reaction mechanism function of the double-base propellant. The mechanisms of the chemical reactions corresponding to the main exothermal decomposition reactions of the control sample and DAG modified propellant are classified, respectively, as $f(\alpha) = \frac{3}{2}(1-\alpha)^{4/3}[(1-\alpha)^{-1/3}-1]^{-1}$ and $f(\alpha) = \frac{5}{2}(1-\alpha)[-\ln(1-\alpha)]^{3/5}$, while their kinetic equations are: $d\alpha/dt = 1.60 \times 10^{17}(1-\alpha)^{4/3}[(1-\alpha)^{-1/3}-1]^{-1} e^{-2.21\times10^4/T}$ and $d\alpha/dt = 9.28 \times 10^{40}(1-\alpha)[-\ln(1-\alpha)]^{3/5} e^{-4.66\times10^4/T}$. Evaluating thermal safety of the propellants samples showed that the DAG modified propellant has a higher resistance to heat and higher thermal safety than the control propellant. Furthermore, DAG could reduce efficiently the pressure exponent of the homogeneous double-base propellant to 0.068 at the pressure of 5–7 MPa.

References

1. Gunasekaran A, Jayachandran T, Boyer JH, Trudell ML. A convenient synthesis of diaminoglyoxime and diaminofurazan: useful precursors for the synthesis of high density energetic materials. J Heterocycl Chem. 1995;32:1405–7.
2. Pourmortazavi SM, Kohsari I, Teimouri MB, Hajimirsadeghi SS. Thermal behaviour kinetic study of dihydroglyoxime and dichloroglyoxime. Mater Lett. 2007;61:4670–3.
3. Komin AP, Street RW, Carmack M. Chemistry of 1,2,5-thiadiazoles. III. [1,2,5] thiadiazolo [3,4-c][1,2,5] thiadiazole. J Org Chem. 1975;40:2749–52.
4. Talawar MB, Sivabalan R, Senthilkumar N, Prabhu G, Asthana SN. Synthesis, characterization and thermal studies on furazan- and tetrazine-based high energy materials. J Hazard Mater. 2004;113:11–25.
5. Kohsari I, Pourmortazavi SM, Hajimirsadeghi SS. Non-isothermal kinetic study of the thermal decomposition of diaminoglyoxime and diaminofurazan. J Therm Anal Cal. 2007;89:543–6.
6. Kanno H, Yamamoto H, US Patent 5,476,967 (1995).
7. Shamsipur M, Pourmortazavi SM, Roushani M, Miran Beigi AA. Thermal behavior and non-isothermal kinetic studies on titanium hydride-fueled binary pyrotechnic compositions. Combust Sci Technol. 2013;185:122–33.
8. Sinditskii VP, Burzhava AV, Chernyi AN, Shmelev DS, Apalkova VN, Palysaeva NV, Sheremetev AB. A comparative study of two difurazanyl ethers. J Therm Anal Calorim. 2016;123:1431–8.
9. Ravanbod M, Pouretedal HR, Catalytic effect of Fe_2O_3, Mn_2O_3, and TiO_2 nanoparticles on thermal decomposition of potassium nitrate. J Therm Anal Calorim. doi:10.1007/s10973-015-5167-y
10. Han Z, Wang D, Wang H, Henkes C. Electrospray formation of RDX/ceria mixture and its thermal decomposition performance. J Therm Anal Calorim. 2016;123:449–55.
11. Takahashi PM, Netto AVG, Mauro AE, Frem RCG. Thermal study of nickel(II) pyrazolyl complexes. J Therm Anal Calorim. 2005;79:335–8.
12. Stoner CE Jr, Brill TB. Thermal decomposition of energetic materials 46. The formation of melamine-like cyclic azines as a mechanism for ballistic modification of composite propellants by DCD, DAG, and DAF. Combust Flame. 1991;83:302–8.
13. Trache D, Khimeche K, Mezroua A, Benziane M, Physicochemical properties of microcrystalline nitrocellulose from Alfa grass fibres and its thermal stability. J Therm Anal Calorim. doi:10.1007/s10973-016-5293-1

14. Pourmortazavi SM, Hosseini SG, Hajimirsadeghi SS, Fareghi Alamdari R. Investigation on thermal analysis of binary zirconium/oxidant pyrotechnic systems. Combus Sci Technol. 2008;180:2093–102.
15. Fathollahi M, Pourmortazavi SM, Hosseini SG. The effect of the particle size of potassium chlorate in pyrotechnic compositions. Combust Flame. 2004;138:304–6.
16. Wei H, Liming H, Zhongliang M, Yanlia G, The kinetic and viscosity analysis of glycidyl azide polymer spherical propellant. J Therm Anal Calorim. doi:10.1007/s10973-015-5225-5
17. Talawar MB, Makashir PS, Nair JK, Pundalik SM, Mukundan T, Asthana SN, Singh SN. Studies on diaminoglyoxime (DAG): thermolysis and evaluation as ballistic modifier in double base propellant. J Hazard Mater. 2005;A 125:17–22.
18. Williams GK, Palopoli SF, Brill TB. Thermal decomposition of energetic materials 65. Conversion of insensitive explosives (NTO, ANTA) and related compounds to polymeric melon-like cyclic azine burn-rate suppressants. Combust Flame. 1994;98:197–204.
19. Park DJ, Stern AG, Willer RL. A convenient laboratory preparation of cyanogen. Synth Commun. 1990;20:2901–6.
20. Pourmortazavi SM, Hosseini SG, Rahimi-Nasrabadi M, Hajimirsadeghi SS, Momenian H. Effect of nitrate content on thermal decomposition of nitrocellulose. J Hazard Mater. 2009;162:1141–4.
21. Yi JH, Zhao FQ, Hong WL, Xu SY, Hu RZ, Chen ZQ, Zhang LY. Effects of Bi-NTO complex on thermal behaviors, nonisothermal reaction kinetics and burning rates of NG/TEGDN/NC propellant. J Hazard Mater. 2010;176:257–61.
22. Kissinger HE. Reaction kinetics in differential thermal analysis. Anal Chem. 1957;29:1702–6.
23. Hu R-Z, Gao S-L, Zhao F-Q, Shi Q-Z, Zhang T-L, Zhang J-J. Thermal Analysis Kinetics. 2nd ed. Beijing: Science Press; 2008.
24. Ma H-X, Song J-R, Hu R-Z. Non-isothermal kinetics of the thermal decomposition of 3-nitro-1,2,4-triazol-5-one magnesium complex. Chin J Chem. 2003;21(12):1558–61.
25. Hu R-Z, Chen S-P, Gao S-L, Zhao F-Q, Luo Y, Gao H-X, Shi Q-Z, Zhao H-A, Yao P, Li J. Thermal decomposition kinetics of $Pb_{0.25}Ba_{0.75}(TNR)\cdot H_2O$ complex. J Hazard Mater. 2005;A117:103–10.
26. Shamsipur M, Pourmortazavi SM, Hajimirsadeghi SS. Investigation on decomposition kinetics and thermal properties of copper fueled pyrotechnic compositions. Combust Sci Tech. 2011;183:575–87.
27. Ma H-X, Song J-R, Zhao F-Q, Hu RZ, Xiao H-M. Nonisothermal reaction kinetics and computational studies on the properties of 2,4,6,8-tetranitro-2,4,6,8-tetraazabicyclo [3,3,1] onan-3,7-dione (TNPDU). J Chem Phys. 2007;A111:8642–9.
28. Starink MJ. The determination of activation energy from linear heating rate experiments: a comparison of the accuracy of isoconversion methods. Thermochim Acta. 2003;404:163–76.
29. Pourmortazavi SM, Hajimirsadeghi SS, Kohsari I, Fathollahi M, Hosseini SG. Thermal decomposition of pyrotechnic mixtures containing either aluminum or magnesium powder as fuel. Fuel. 2008;87:244–51.
30. Shamsipur M, Pourmortazavi SM, Hajimirsadeghi SS, Atifeh SM. Effect of functional group on thermal stability of cellulose derivative energetic polymers. Fuel. 2012;95:394–9.
31. Tompa AS, Boswell RF. Thermal stability of a plastic bonded explosive. Thermochim Acta. 2000;357–358:169–75.
32. ASTM E698-11, standard test method for arrhenius kinetic constants for thermally unstable materials using differential scanning calorimetry and the Flynn/Wall/Ozawa method, ASTM international, west conshohocken, PA, 2011. http://www.astm.org.
33. Shamsipur M, Pourmortazavi SM, Fathollahi M. Kinetic parameters of binary iron/oxidant pyrolants. J Energy Mater. 2012;30:97–106.
34. Pickard JM. Critical ignition temperature. Thermochim Acta. 2002;392:37–40.
35. Tompa AS, Boswell RF. DSC and TG study of the stability in vacuum of ferrocenyl compounds and their compatibility with ammonium perchlorate. Thermochim Acta. 1984;77:133–50.
36. Boldyrev VV. Thermal decomposition of ammonium perchlorate. Thermochim Acta. 2006;443:1–36.
37. Chen P, Zhao F-Q, Luo Y, Hu R-Z, Gao S-L, Zheng Y-M, Deng M-Z, Gao Y. Thermal decomposition behavior and non-isothermal decomposition reaction of copper(II) salt of 4-hydroxy-3,5-dinitropyridine oxide and its application in solid rocket propellant. J Chem. 2004;22:1056–63.
38. Yi J-H, Zhao F-Q, Wang B-Z, Liu Q, Zhou C, Hu R-Z, Ren Y-H, Xu S-Y, Xu K-Z, Ren X-N. Thermal behaviors, nonisothermal decomposition reaction kinetics, thermal safety and burning rates of BTATz-CMDB propellant. J Hazard Mater. 2010;181:432–9.
39. Yi J-H, Zhaoa F-Q, Xu S-Y, Zhang L, Gao H, Hu R-Z. Effects of pressure and TEGDN content on decomposition reaction mechanism and kinetics of DB gun propellant containing the mixed ester of TEGDN and NG. J Hazard Mater. 2009;165:853–9.
40. Weijian N, Xiaopeng C, Linlin W, Jiezhen L, Lingping Z, Zhangfa T. Thermal decomposition kinetics of abietic acid in static air. Chin J Chem. 2013;21(7):724–9.
41. Chen KY, Wu SH, Wang YW, Shu CM. Runaway reaction and thermal hazards simulation of cumene roperoxide by DSC. J Loss Prevent Proc. 2008;21:101–9.